Materials and Design 64 (2014) 324–329

Contents lists available at ScienceDirect

Materials and Design

journal homepage: www.elsevier.com/locate/matdes

Processing of magnesium foams by weakly corrosive and highly flexible space holder materials

Xingfu Wang, Zhendong Li, Yingjie Huang, Kun Wang, Xinfu Wang, Fusheng Han *

Key Laboratory of Materials Physics, Institute of Solid State Physics, Chinese Academy of Sciences, Hefei, Anhui 230031, China

ARTICLE INFO

Article history:
Received 5 May 2014
Accepted 23 July 2014
Available online 4 August 2014

Keywords:
Magnesium foams
Infiltration process
Mechanical properties
Tunable pore structures

ABSTRACT

High-quality magnesium foams were fabricated by an infiltration technology using tailor-made salt–flour mixture space holders. The pore structures and mechanical properties of space holder particles as well as the resultant foam production with spherical pores were characterized in the present study. The particles after high-temperature sintering dissolved rapidly in water due to their porous structures, guaranteeing the weak corrosion and high-purity of magnesium foams. The spherical pores foams exhibited usual stress–strain behaviors and nearly isotropic properties. The yield strengths of the foams increased with the decrease of sample porosity, and the relative mechanical properties of foams were mostly dependent on their relative densities, which obeyed a power law relation. Moreover, porous magnesium materials with tunable pore structures could be fabricated owing to the flexible forming features of salt–flour mixture, showing great application prospects in bone implant material field.

1. Introduction

Magnesium (Mg) foams have drawn much attention as promising biodegradable bone implant materials due to their outstanding biocompatibility, favorable mechanical properties and similar porous structures close to that of natural bones [1]. In order to produce Mg foams suitable for bone implants, many techniques have been developed including powder metallurgy [2–7], molten metal infiltration [8–12], metal foaming [13,14], metal/gas eutectic unidirectional solidification method [15], and so on. These technologies do have yielded Mg foams with a variety of pore structures and desired properties, but there still exist limitations and shortcomings. For example, in the first two approaches, the residues of resolvable space holders or porous preform materials are usually inevitable in the cell walls that give rise to the pollution and deteriorated physical/chemical properties of Mg foams. Wen et al. found that a little amount of carbon remained on the cell wall surface of Mg foams when preparing them using carbamide particles as the space holder [2]. However, the carbon residues would seriously impair the biocompatibility of the foams [1]. Moreover, even though with the same porosity the Mg foams showed noticeably different compressive flow stresses in the plateau region due to the uneven distribution of the different sized pores in the samples [3]. In order to overcome these shortcomings, Hao et al. used round-shaped carbamide particles to substitute those polygonal ones and introduced a preliminary low-temperature consolidation and dissolution process prior to high-temperature sintering [4]. This process effectively eliminated the residues of space holder particles in the cell walls and improved the quality of Mg foams. However, the foams still presented brittle characteristics.

High-quality metal foams have often been obtained through infiltration technology. In the molten metal infiltration process for fabricating aluminum foams, NaCl (crude salt) particles are the most widely used preform material [16]. However, this material would be unsuitable for the preparation of Mg foams because of its strong corrosion effect as well as the high chemical activity of Mg matrix. Hence, it is necessary to find other preform materials of weak corrosiveness or shorten the dissolution time of preform to reduce the corrosion of Mg matrix. Xu et al. [10] adopted $MgSO_4$ to substitute NaCl in fabricating Mg foams via infiltration process and found that the corrosion of Mg matrix was reduced indeed, but the dissolution time was not obviously shortened, which was not suitable for the fabrication of large-scale Mg foam samples. Staiger et al. utilized 3D net shaped polymeric materials as the cell wall pattern filled with NaCl paste to prepare topologically-ordered Mg foams through burning-out the polymer, sintering the NaCl particles and infiltrating molten Mg [11,12]. The resultant Mg foams had very high purity and underwent quite weak corrosion due to quick dissolution of NaCl preform. These researches

* Corresponding author. Tel.: +86 551 5591435; fax: +86 551 5591434.
E-mail address: fshan@issp.ac.cn (F. Han).

http://dx.doi.org/10.1016/j.matdes.2014.07.049
0261-3069/

demonstrate that the employment of easily soluble space holders is an effective way to fabricate high-purity Mg or Mg alloy foams. In consideration of biomedical applications, it is of great value to obtain open-cell Mg foam with superior purity to ensure its biocompatibility and predictable mechanical performance to fulfill required load bearing functions during the implantation period. Although the Mg foams produced by the aforementioned metal foaming and metal/gas eutectic unidirectional solidification technologies have no harmful residues, they are not suitable for bone implants due to the inconsistent morphologies with closed cell structures [1,13,14].

Recently, a new method has been developed in fabricating aluminum foams using a soluble mixture of flour and salt powder as the space holder [17]. The preform can easily and quickly dissolve in water after the infiltration and thus should be also appropriate for fabricating Mg foams. The other advantage is the flexible shapes of space holder due to the easy forming characteristics of flour, being very beneficial to providing the metal foams with different pore structures and mechanical properties. Therefore, this technology was utilized in the present study with the objective of processing Mg foams with high-purity, spherical pores and favorable properties. The results are expected to provide useful information for the further studies on the development of Mg foams and their applications in the bone implant field.

2. Experimental details

Spherical salt–flour mixture particles were produced by granulation method [18], and the process is outlined schematically in Fig. 1. Specifically, crude salt was pulverized and then classified through a 200-mesh sieve. The resultant salt powders (powder size $\leqslant$74 μm) and comparable sized flour with different contents (5, 10, 15 and 20 percent in weight ratio) were evenly mixed together. Finally, the spherical salt–flour mixture particles were acquired on a pan-type pelletizer utilizing spray water as the binder. After that, the spherical particles with the average diameter of 1.6 mm were obtained by sieving and then heated to 680 °C for 2 h in air atmosphere to make the water volatilize and flour pyrolyze. Thus, the additives could be removed, which left behind the salt particles with high porosity (refer to Fig. 2a and b). The preform was subsequently prepared by stacking a number of salt particles under an appropriate axial compression in a cylindrical mould.

Mg foam was prepared by infiltrating molten Mg into salt preform followed by the dissolution of salt in ingot. Specifically, Mg ingot (99.7% purity) was placed on top of the mould and vacuum was pulled to 4×10^{-2} mbar residual pressure, and then the mould was heated to 680 °C for 1 h before molten Mg was infiltrated into the preform using argon pressurized to 0.1 MPa. After solidification, the ingot was taken out and machined to the desired dimension prior to the removal of salt in 0.001 M NaOH water solution. The morphology of the resultant production is presented in Fig. 2c. The porosity of the sample was determined by the equation.

$$P = (1 - \rho_0/\rho_s) \quad (1)$$

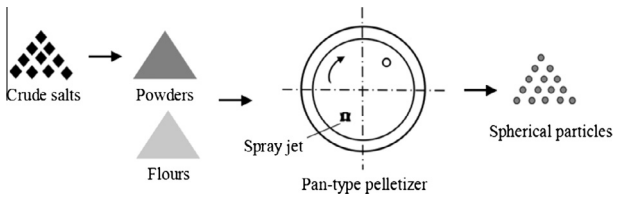

Fig. 1. Schematic illustration of the process for fabricating spherical salt–flour mixture particles.

where ρ_0 is the apparent density of the sample determined by its dimension and weight, and ρ_s is the density of Mg. The open porosity P_0 was estimated by the Archimedes method.

$$P_0 = (V_s - V_d)/V_s \quad (2)$$

where V_s and V_d are the samples' volume and drained water volume respectively.

The dissolution rate of spherical salt particles was characterized via an immersion test: 1 g specimen was immersed in 30 mL water and the crude salt was exerted for comparison. The morphologies of salt particles and foams were characterized on a field-emission scanning electron microscope (FE-SEM, FEI Sirion 200), and the surface profile of Mg foam was analyzed by EDS microanalysis system attached to FE-SEM. The compressive tests for salt preform and resultant foams were performed using an Instron 3369 materials testing system with a crosshead speed of 2 mm/min. The samples for the compressive tests were 20 mm in diameter and 20 mm in height. The elastic modulus of Mg foams were calculated on the basis of curves fitted to the linear elastic regions of the stress–strain curves and yield strength values were determined using the 0.2%-offset method.

3. Results and discussion

3.1. The structure and properties of spherical salt particles

Typical structure of salt–flour mixture particles fabricated by granulation method is shown in Fig. 2a. The particles are nearly spherical in shape and vary in size, and the diameter of the particle is centered largely in the range of 1.4–1.6 mm. The particles with desired size could be acquired by the optimization of granulation parameters. It was pointed out that the binder content and rotational speed as well as granulation time could affect the size distribution of granules [18]. In order to enhance the efficiency of granulation, the short granulation time (5 min), high rotational speed (240 rpm) and the appropriate spraying water (about 0.1 mm in diameter) were determined to fabricate spherical salt–flour mixture particles in the study. As can be seen from Fig. 2b, the single salt particle after high-temperature sintering appears obviously vesicular structure, except for the numerous cavities in spheroid mainly given by the volatilization of water and the burning-out of flour, the other reason could be attributed to the granulation process itself that combined fine powders into larger agglomerates without forming pressure, this would inevitably lead to the loose packing of salt–flour mixture powders (refer to the high magnification image inserted in Fig. 2b).

The dissolution rates of crude salt and spherical salt particles in water were characterized by immersion experiments. The time required for crude salt to dissolve was more than 15 min, while the complete dissolution of spherical salt particles with different flour adding (5 wt.%, 10 wt.%, 15 wt.%, 20 wt.%) were about 45, 25, 20 and 20 s respectively. The dissolution rate of salt particles enhances with the increase of flour adding due to their high porosity, which was formed by the loose aggregation of fine salt–flour mixture powders, the volatilization of water as well as the flour pyrolysis. It was validated from Fig. 3a–d that many pores formed in the salt particles after high-temperature sintering. As observed from the image inserted in Fig. 3a that many sintering necks emerged on the border of interparticle contacts. Moreover, the densification was obviously discovered through visualized volume shrinkage after sintering. It was stated that boundary diffusion would dominate the sintering of NaCl powders with the size below 150 μm and lead to densification [19]. Therefore, the formation of sintering necks should be attributed to the boundary diffusion among fine salt powders. The prediction has been confirmed by

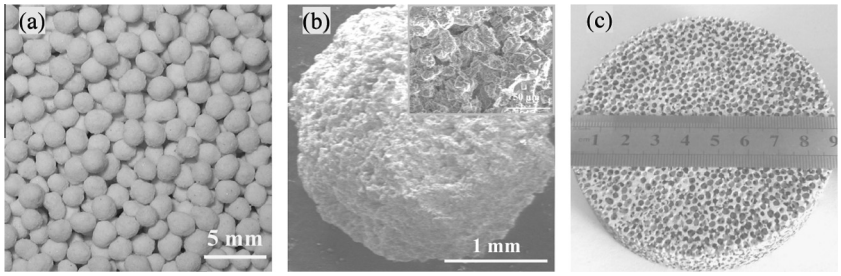

Fig. 2. (a) Photograph of spherical salt–flour mixture particles, (b) morphology of a single salt particle and (c) FE-SEM image of Mg foam.

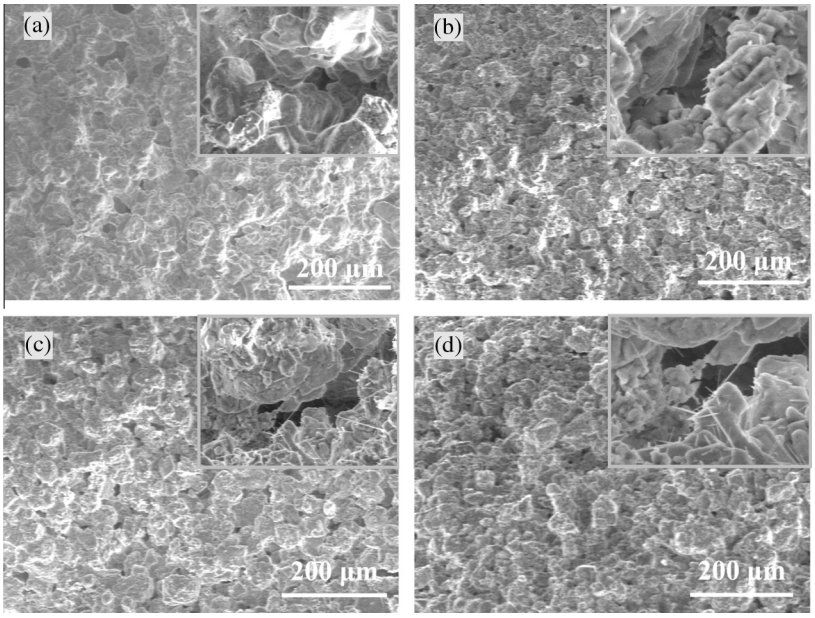

Fig. 3. FE-SEM images of salt particles processed with different flour adding (a) 5 wt.%, (b) 10 wt.%, (c) 15 wt.%, (d) 20 wt.%.

Gokhale et al., who carried out a sintering experiment on iron powders and further revealed that the number of interparticle contacts was mainly determined by the initial stacking state of fine powders [20]. Hence, the conclusion of this study could be drawn that the aggregation state of fine salt–flour mixture powders was the deciding factor for the number of sintering necks. Thus, with the increase of flour adding, the density of salt powders aggregation decreases, and the number of interparticle contacts becomes less after sintering, which would finally inhibit the boundary diffusion (refer to Fig. 3b–d). So it is easy to infer that the greater flour adding in salt–flour mixture particles, the higher porosity of the final object has, and the more penetrating channels between the water and salt particle hold, hence the water can easily penetrate into salt particles and make them dissolve accelerative.

As the flour adding in salt–flour mixture particles enhances to 20 wt.%, a few fibrous materials formed on the edge of the interparticle contacts (refer to the image inserted in Fig. 3d) after sintering, this was possibly due to the incomplete burning-out of flour, which would exert a deleterious affect on the dissolution rate and mechanical property of salt preform.

In order to get an extensive knowledge of salt preform to determine its stacking state, compressive tests were carried out and the stress–strain curves are shown in Fig. 4. A linear rise in stress can be observed at the initial stage and a short plateau emerges at the strain point of 2%, here the weight ratio of unbroken salt to starting value of four salt preforms are 98.5%, 96.8%, 95.6% and 97.1% respectively. The values of broken ratio are quite low which

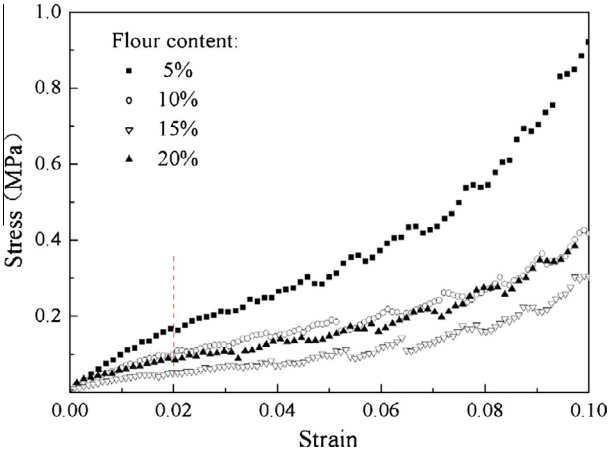

Fig. 4. Stress–strain curves of spherical salt particles.

indicated that the initial strain was mainly caused by the plastic deformation of salt particles. Therefore, the precompression towards salt particles in a cylindrical mould for preform preparation was settled at 2% straining. The following increase in stress was accompanied by the crush of salt particles, this was confirmed by the compressive tests till 10% in strain: the unbroken ratio dipped to 65%, 62.8%, 59.5% and 61.3% correspondingly. Compared with the four curves, the stress of the salt particles decreases with

the increase of flour adding, but an abnormal phenomenon was observed on the salt preform processed with 20 wt.% flour adding, this could be due to the incomplete burning-out of flour which improved its compressive strength.

3.2. The structure and properties of Mg foams

A series of parameters, such as pore size, cell wall thickness, porosity and open porosity have been used to characterize the Mg foam structure in the study. As shown in Fig. 5a, the foams were discovered to contain mainly two types of pores: the macropores obtained as a result of the dissolution of salt particles and the small pores derived from the interparticle contacts. The small pores usually distributed on the cell center, generating the connection tunnels among macropores, which made the foams present very high open porosity (99%). The cell wall (the border region of two macropores) thickness was in the range of 0.2–0.6 mm, showing a great amount of fluctuations, and the cell edge (refer to Fig. 5a) surrounded by more than two pores have similar nonuniformity in dimension, which would lead to some difficulties in performance simulations. The macropore diameter (D) was about 1.5 mm, slightly smaller than the average diameter of primary salt–flour mixture particles, this could be induced by the particle densification occurred in sintering process. The small pore diameter (d) was in the range of 0.6–0.9 mm, as has been reported by our group [21], the value of d was mainly determined by the infiltration pressure, the salt particle radius and the wetting angle between the liquid magnesium and the salt particles as the packing density of salt preform is constant. Thus, it could be deduced that the infiltration parameters play a critical role on the connectivity of Mg foams, which would also provide great flexibility for the structural design of spherical pores Mg foams. Fig. 5b shows the EDS profile of Mg and O for porous Mg sample, no Cl or other elements were detected, this suggested that there was no chemical reaction occurred during the infiltration process, showing a very promising application prospect as biodegradable bone implant materials. A small amount of O was observed on the cell wall, this was probably due to the surface oxidation of foams stored at room temperature.

Except for the structure analysis, the mechanical properties of Mg foams which should match with the target substitution need to be studied and the results of Mg foams for compressive tests are shown in Fig. 6. It is found that the curves exhibit similar trend and present usual compressive properties of metallic foams [4], that is, an elastic stage at the beginning, a quite long plateau region with a nearly constant stress and a densification stage where the stress rapidly increases. Unlike the properties of samples produced by powder metallurgy method, which appear obvious brittle nature, the porous Mg with spherical pores in the study exhibits a typical elastic–plastic deformation characteristic due to the excellent metallurgical quality given by the infiltration technology. It has been noted that cell edge bending is the dominant mechanism that controls the linear elasticity; the plateau is associated with the buckling and collapse of cell walls; and the subsequent increase in stress is a consequence of the compression of solid itself after complete collapsing of cells [22]. As observed in Fig. 6a, the two foam samples machined from the same ingot along different directions have similar porosity and mechanical property, showing nearly isotropic characteristics. However, it is noteworthy that two curves appear a bit difference: sample 2 machined along the transverse direction has higher yield strength and longer plateau region, this could be caused by the plastic deformation of salt preform after 2% straining axial compression that finally led to the pore elongation at transverse direction in the ingot, which would increase the buckling and collapse range of the cell walls. Mg foams with different porosity by varying the compression amount towards salt preform were acquired and the effect of porosity on the mechanical property was studied. It is evident from Fig. 6b that the yield strength of Mg foam increases with the decrease of porosity. As discussed by Gibson and Ashby [22], cell edge bending dominated the linear elasticity during the first stage of deformation, thus, it could be deduced that as the porosity decreases, the value of the cell edge raises, finally resulting in the increase of yield strength. As mentioned above, the cell wall thickness of foams presents inhomogeneous feature and the initial loading curves in Fig. 6 are not exactly linear, leading to mechanical properties that are lower than expected. The reason could be ascribed to the weakest cell wall which would act as the nuclei of buckling formation for the initiation of strain localization [4,23]. As the uniaxial compression proceeds, the deformation propagates through the foam, finally resulting in a band of collapsed cells. As the porosity of the sample decreases, the plateau region becomes narrowed and the stress after yielding increases relatively rapidly, the phenomenon was obviously observed in the samples 3–5. Concretely, the yield strengths of Mg foams containing porosities in the range 54.4–70.4% vary between 3.57 and 8.65 MPa, and the resultant elastic modulus are between 20.6 and 50 MPa, which are in the range of mechanical properties of cancellous bone [2]. Many empirical relations obtained by a best fit to the experimental data and theoretical relations have been proposed to describe the dependence of the mechanical properties of foams on their porosities [22,23]. Gibson and Ashby put forward a modest bending strut model and deemed that the strength of foam is linearly dependent on the relative density [22]. However, this model is only valid for the cellular solids with relative densities of less than 0.3. Esen and Bor studied the dependence of relative mechanical properties of titanium foams on their relative densities and revealed that they obeyed a power law relation [23]. In the present study, the dependence of the relative yield strength (σ_0/σ_s) and relative Young's modulus (E_0/E_s) of Mg foams on their relative densities (ρ_0/ρ_s) was observed to be in conformity with Esen's conclusion, as shown by the fitted line in Fig. 7, where a density of 1.74 g/cm^{-3}, yield strength of 21 MPa and Young's modulus of 40 GPa are used as

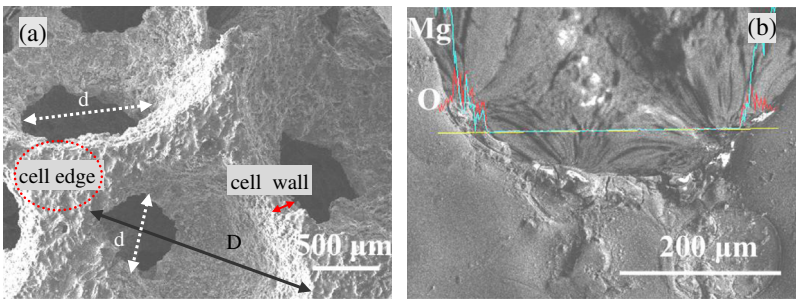

Fig. 5. (a) FE-SEM image of Mg foam with the porosity of 64% and (b) EDS profile of Mg (84.73 wt.%) and O for foam (15.27 wt.%) samples.

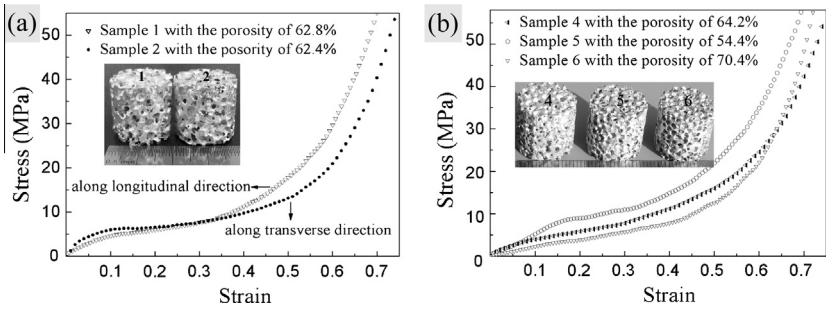

Fig. 6. (a) Stress–strain curves of two Mg foam samples machined along longitudinal and transversal directions and (b) effect of porosity on the mechanical properties of Mg foams.

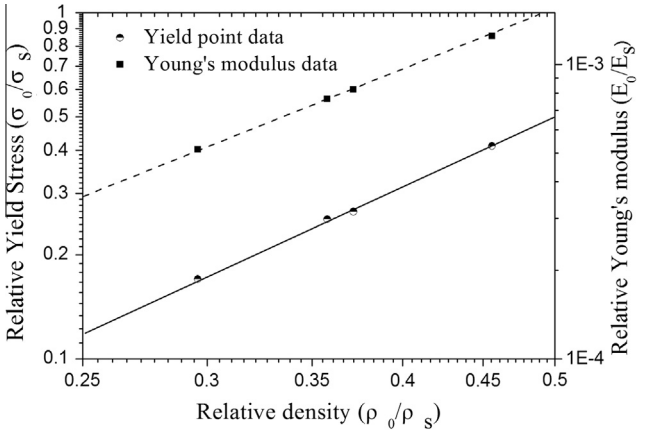

Fig. 7. Change of relative Young's modulus and yield strength with relative density.

the bulk properties of pure Mg in calculating the relative properties:

$$E_0/E_s = 0.006(\rho_0/\rho_s)^{2.05} \quad (R^2 = 0.9994) \tag{3}$$

$$\sigma_0/\sigma_s = 2.068(\rho_0/\rho_s)^{2.06} \quad (R^2 = 0.9985) \tag{4}$$

While the proportionality constant and the exponent might reflect the foam parameters, such as pore morphology, shape and arrangement of the cell walls. Moreover, various Mg foams with tunable pore structures can be acquired through the construction of salt–flour mixture space holders permitted by the easy forming characteristics of flour. For instance, lotus-type porous Mg (refer to Fig. 8a) was fabricated based on a stacking of noodle-shaped space holders using a handmade noodle maker (see Fig. 8b). Therefore, in the present study, Mg foam productions have great flexibility in regulation of structure and properties, showing abroad application prospects as bone implant materials.

4. Conclusions

A weakly corrosive and highly flexible salt–flour mixture space holder material was developed for fabricating Mg foams by a molten metal infiltration process. The results show that the space holder particles have high dissolution rate, making the resultant foams exhibit high-quality without harmful residues in the cell walls. The foams presented usual stress–strain behaviors and good mechanical properties, depending on the porosities or the relative densities of the foam samples. The shapes of the space holder material can be tailored to yield varied pore structures and properties of Mg foams to meet the needs of practical applications.

Acknowledgments

This work was supported by the National Science Foundation of China (51301168 and 51371167), the National Basic Research Program of China (2011CB610300) and the Instrument Developing Project of the Chinese Academy of Sciences (YG2012065).

References

[1] Staiger MP, Pietak AM, Huadmai J, Dias G. Magnesium and its alloys as orthopedic biomaterials: a review. Biomaterials 2006;27:1728–34.
[2] Wen CE, Yamada Y, Shimojima K, Chino Y, Hosokawa H, Mabuchi M. Compressibility of porous magnesium foam: dependency on porosity and pore size. Mater Lett 2004;58:357–60.
[3] Wen CE, Mabuchi M, Yamada Y, Shimojima K, Chino Y, Asahina T. Processing of biocompatible porous Ti and Mg. Scripta Mater 2001;45:1147–53.
[4] Hao GL, Han FS, Li WD. Processing and mechanical properties of magnesium foams. J Porous Mater 2009;16:251–6.
[5] Hao GL, Han FS, Wu J, Wang XF. Mechanical and damping properties of porous AZ91 magnesium alloy. Powder Metall 2007;50:127–31.
[6] Zhuang HY, Han Y, Feng AL. Preparation, mechanical properties and in vitro biodegradation of porous magnesium scaffolds. Mater Sci Eng C Biomim Supramol Syst 2008;28:1462–6.
[7] Capek J, Vojtech D. Properties of porous magnesium prepared by powder metallurgy. Mater Sci Eng C Mater Biol Appl 2013;33:564–9.
[8] Yamada Y, Shimojima K, Sakaguchi Y, Mabuchi M, Nakamura M, Asahina T, et al. Processing of an open-cellular AZ91 magnesium alloy with a low density of 0.05 g/cm^3. J Mater Sci Lett 1999;18:1477–80.

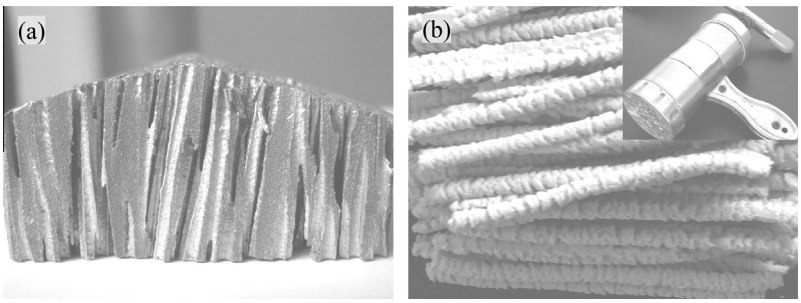

Fig. 8. Photograph of lotus-type porous Mg (a) and noodle-shaped space holders (b).

[9] Ho S, Ravindran C, Hibbard GD. Magnesium alloy micro-truss materials. Scripta Mater 2010;62:21–4.
[10] Xu JH, Mao GB, Cheng LP, Hu ZhQ. The study on the vacuum infiltration casting of foam Mg alloy. Jiangxi Metall 2003;23:84–7.
[11] Kirkland NT, Kolbeinsson I, Woodfield T, Dias GJ, Staiger MP. Synthesis and properties of topologically ordered porous magnesium. Mater Sci Eng B Adv Funct Solid-State Mater 2011;176:1666–72.
[12] Staiger MP, Kolbeinsson I, Kirkland NT, Nguyen T, Dias G, Woodfield TBF. Synthesis of topologically-ordered open-cell porous magnesium. Mater Lett 2010;64:2572–4.
[13] Xia XC, Zhao WM, Feng XZ, Feng H, Zhang X. Effect of homogenizing heat treatment on the compressive properties of closed-cell Mg alloy foams. Mater Des 2013;49:19–24.
[14] Xu ZG, Fu JW, Luo TJ, Yang YS. Effects of cell size on quasi-static compressive properties of Mg alloy foams. Mater Des 2012;34:40–4.
[15] Gu XN, Zhou WR, Zheng YF, Liu Y, Li YX. Degradation and cytotoxicity of lotus-type porous pure magnesium as potential tissue engineering scaffold material. Mater Lett 2010;64:1871–4.
[16] San Marchi C, Mortensen A. Deformation of open-cell aluminum foam. Acta Mater 2001;49:3959–69.
[17] Goodall R, Mortensen A. Microcellular aluminium? Child's play! Adv Eng Mater 2007;9:951–4.
[18] Sochon RPJ, Dorvlo SK, Rudd AI, Hayati I, Hounslow MJ, Salman AD. Granulation of zinc oxide. Chem Eng Res Des 2005;83:1325–30.
[19] Goodall R, Despois JF, Mortensen A. Sintering of NaCl powder: mechanisms and first stage kinetics. J Eur Ceram Soc 2006;26:3487–97.
[20] Gokhale AM, Basavaiah M, Upadhyaya GS. Kinetics of neck growth during loose stack sintering. Metall Trans A Phys Metall Mater Sci 1988;19:2153–61.
[21] Li YJ, Wang XF, Wang XF, Ren YL, Han FSh, Wen CE. Sound absorption characteristics of aluminum foam with spherical cells. J Appl Phys 2011;110:113525.
[22] Gibson LJ, Ashby MF. Cellular solids structure and properties. Cambridge university press; 1997.
[23] Esen Z, Bor S. Processing of titanium foams using magnesium spacer particles. Scripta Mater 2007;56:341–4.